
Cross-Service Threat Intelligence in LLM Services using Privacy-Preserving Fingerprints

Waris Gill
Microsoft
Redmond, WA

Natalie Isak
Microsoft
New York, NY

Matthew Dressman
Microsoft
Redmond, WA

Abstract

The widespread deployment of LLMs across enterprise services has created a critical security blind spot. Organizations operate multiple LLM services handling billions of queries daily, yet regulatory compliance boundaries prevent these services from sharing threat intelligence about prompt injection attacks, the top security risk for LLMs. When an attack is detected in one service, the same threat may persist undetected in others for months, as privacy regulations prohibit sharing user prompts across compliance boundaries.

We present *BinaryShield*, *the first privacy-preserving threat intelligence system that enables secure sharing of attack fingerprints across compliance boundaries*. *BinaryShield* transforms suspicious prompts through a unique pipeline combining PII redaction, semantic embedding, binary quantization, and randomized response mechanism to potentially generate non-invertible fingerprints that preserve attack patterns while providing privacy. Our evaluations demonstrate that *BinaryShield* achieves an F1-score of 0.94, significantly outperforming SimHash (0.77), the privacy-preserving baseline, while achieving 64x storage reduction and 38x faster similarity search compared to dense embeddings.

1 Introduction

The rapid adoption of Large Language Models (LLMs) in digital services is driving a paradigm shift in human-computer interaction. Companies now operate many LLM-based services across diverse domains, collectively handling billions of queries each day. Typically, organizations like Microsoft maintain multiple, logically isolated (siloed) LLM services, such as enterprise AI assistants, consumer chat applications, API based LLM services, and developer-focused coding agents. These services are siloed because they are tailored to meet distinct business objectives and end-user requirements, necessitating separate operational boundaries. Each service has distinct model stacks, logging pipelines, and compliance boundaries with strong internal data governance policies to protect user data and privacy. In addition to internal privacy regulations, these services are also subject to governmental regulations such as GDPR and HIPAA, which mandate strict data handling practices to protect user privacy and sensitive information. While this siloed architecture is crucial for maintaining operational independence, it has an unintended consequence: fragmented security telemetry and a weakened collective defense. With little correlation or data sharing between services, organizations are left with a disjointed security posture as each service operates independently, responding to threats in isolation. *This fragmentation creates a significant challenge for incident response teams, as they lack a unified view of the threat landscape across their LLM services.*

Prompt Injection and Current Defenses. The new interaction model, based on natural language prompts, introduces a critical security risk: prompt injection attacks. Often described as the “SQL injection” of AI, prompt injection is recognized as the top threat in the OWASP 2025 Top 10 for LLMs. Prompt injection exploits LLMs’ inability to distinguish legitimate user instructions from

malicious commands embedded in input. These attacks can manipulate system prompts to leak private data, execute malicious code via tool interfaces, or generate harmful content. With emerging technologies like Model Context Protocol (MCP) servers and autonomous agents, the impact of prompt injection extends beyond text manipulation to arbitrary code execution and potential system compromise [News]. Organizations and researchers have developed various defense mechanisms against these attacks [Abdelnabi et al., 2025a,b]. Furthermore, more than one defenses are deployed to enhance security within a compliance boundary [Abdelnabi et al., 2025b]. However, a critical limitation stems directly from privacy regulations that prevent the sharing of user prompts between compliance boundaries (i.e., services). These regulations force each defense mechanism to operate in isolation, which in turn hinders cross-service threat intelligence and limits visibility.

Motivation and Problem Statement. The current defense paradigm is compartmentalized, with each service responding independently to detected attacks. When a new attack vector is identified (typically through media reports, user complaints, or post-breach analysis) security teams patch their systems (e.g., update prompts classifiers). However, this knowledge remains confined to the affected service. Furthermore, attacks are inevitable because existing defenses are probabilistic and can be bypassed [Debenedetti et al., 2025, Costa et al., 2025]. Thus, organizations need retrospective systems to pinpoint the perpetrator and timing of incidents.

This reactive, siloed approach prevents organization-wide visibility into the threat landscape. An attack discovered in one service today may have existed undetected in another for months. Security analysts lack tools to search for similar historical attack patterns across service boundaries, creating a “correlation gap”. As a result, they cannot fully assess the scale and sophistication of an attack, identify its variants, or proactively protect all services from emerging threats. Traditional malware defense addressed similar coordination challenges decades ago by exchanging signatures: antivirus engines share hash or pattern-based fingerprints of malicious binaries without revealing proprietary information [Li et al., 2019]. To our knowledge, no comparable, privacy-preserving, and practically deployable threat intelligence mechanism exists for natural-language prompts in LLM services. This paper addresses the following problem: *How can an organization securely share threat intelligence about prompt injection attacks across its compliance boundaries without violating privacy regulations?*

Ideal Characteristics of an Attack Fingerprint Technique. A privacy-preserving fingerprinting mechanism for prompt injection attacks is essential for secure information sharing across compliance boundaries. Such a fingerprint must encode the semantic core of the malicious prompt, capturing its essential characteristics beyond surface tokens. It should be computationally non-invertible, preventing even white-box adversaries from reconstructing the original input. The technique must support secure approximate matching for “find-similar” searches across data stores and remain lightweight for real-time generation and distribution. When an attack is detected in one service, the fingerprint can be broadcast to peer services. These peers can then search historical logs for related incidents, flag live traffic, and train local defenses, enabling proactive, collaborative security. Cross-boundary threat intelligence will enable faster patching without compromising user privacy.

Our Contributions. We propose the concept of *threat intelligence* across compliance boundaries in LLM services. We materialize this idea in **BinaryShield**, the first privacy-preserving fingerprinting technique for prompt injection attacks that enables secure information sharing between otherwise siloed services. When a potential threat (prompt injection) is detected within any service by its defense mechanism, **BinaryShield** generates a non-reversible, lightweight fingerprint that distills the semantic essence of the malicious prompt, making it possible to share actionable threat signals while preserving privacy.

Our approach balances the need for threat intelligence sharing with user privacy and regulatory compliance. **BinaryShield** achieves this through a multi-stage process that progressively removes identifying information while retaining the essential semantic characteristics for effective threat detection. The process begins with personally identifiable information (PII) redaction, where **BinaryShield** removes sensitive data such as social security numbers, names, and other identifying markers from input prompts. This initial privacy layer is crucial for protecting users whose prompts may be incorrectly flagged as malicious by automated defenses. However, PII redaction alone is insufficient, as the remaining text may still contain contextual information that could compromise user privacy when shared externally. To capture the semantic essence of potentially malicious prompts, **BinaryShield** generates high-dimensional embeddings from the *redacted text*. These embeddings,

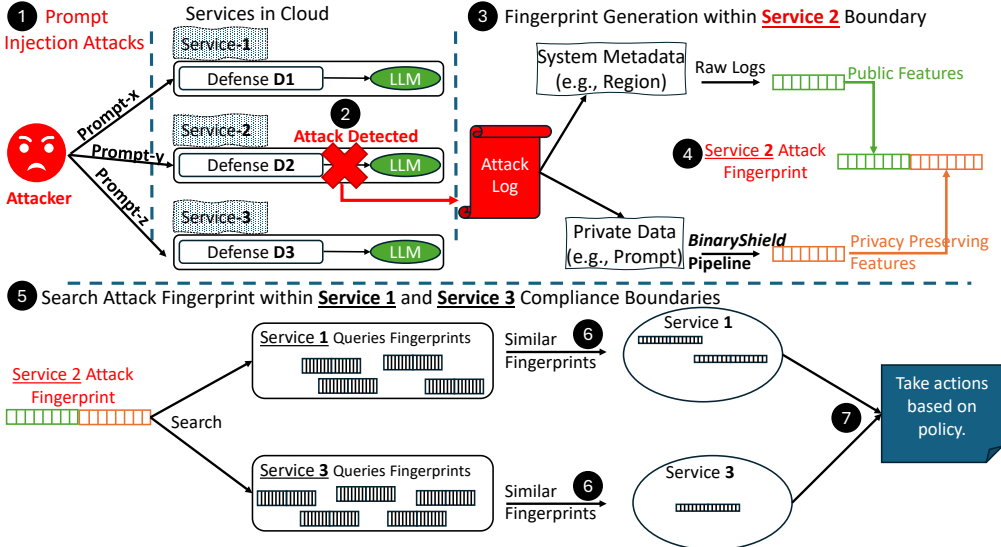


Figure 1: BinaryShield system design. Suspicious prompts are processed within the compliance boundary to generate privacy-preserving fingerprints, which are then shared across services for collaborative threat detection.

which represent text as dense floating-point vectors, achieve state-of-the-art performance in natural language processing tasks by encoding semantic relationships in vector space. However, embeddings are not secure for sharing across compliance boundaries. Recent research demonstrates that embeddings pose significant privacy risks, as they can allow adversaries to reconstruct original input text [Walsh, Li et al., 2023, Tragoudaras et al., 2025, OWASP2025, 2025]. Moreover, traditional embeddings present practical challenges for large-scale threat intelligence system. Each dimension typically requires 32 bits of storage, and similarity computations using cosine similarity or dot products demand substantial computational resources, often necessitating GPU acceleration for efficient threat matching.

BinaryShield addresses these fundamental challenges through two innovative non-reversible transformations by exploiting insights from quantization and differential privacy. First, BinaryShield performs binary quantization on the floating-point embeddings, converting each dimension to a single bit based on its sign, assigning 1 for positive values and 0 for negative values. This quantization achieves remarkable efficiency gains, reducing storage requirements while simultaneously enhancing privacy. The key insight underlying this approach is that by discarding magnitude information and retaining only directional information, we make prompt reconstruction exponentially more difficult while preserving sufficient semantic structure for threat sharing and detection. To render original prompt reconstruction practically impossible, BinaryShield applies differential privacy to the binary embeddings. Leveraging the insights from the principle of randomized response [Warner, 1965, Erlingsson et al., 2014, Wang et al., 2017], BinaryShield independently flips each bit of the binary vector with a precisely calibrated probability. This noise addition fundamentally alters the binary vector representation while preserving its calibrated utility for threat correlation, ensuring that adversaries cannot reverse-engineer the original prompt from the shared fingerprint. The resulting binary vector is efficient in storage and computation, enabling rapid Hamming distance similarity checks. More importantly, after these privacy-preserving transformations, the resulting binary vector becomes safe to share across compliance boundaries, enabling effective cross-service threat intelligence without compromising user privacy or regulatory compliance.

Evaluations. We conduct comprehensive evaluation of BinaryShield spanning threat correlation effectiveness, privacy calibration, scalability, and operational efficiency (Section 3). BinaryShield significantly outperforms privacy-preserving baseline across attack variants (17-point F1 advantage on sophisticated attacks) and exhibits smooth privacy-utility trade-offs with theoretical noise alignment. In real-world enterprise-scale scenarios, BinaryShield achieves 79.2% threat correlation accuracy

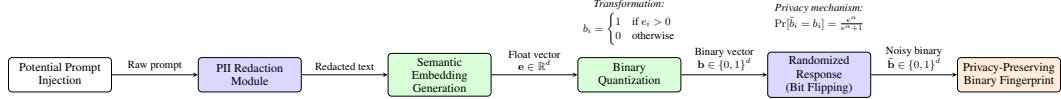


Figure 2: **BinaryShield** approach for privacy-preserving fingerprint generation for cross-service threat intelligence sharing. The pipeline progressively transforms potential prompt injections through PII redaction, semantic embedding, binary quantization, and differential privacy to produce shareable fingerprints that preserve privacy while enabling threat correlation across compliance boundaries.

(93% of non-private baseline performance) alongside efficiency gains (38x search speedup, 64x storage reduction).

2 BinaryShield Design

The proliferation of LLM-based services within organizations creates a fundamental tension between security effectiveness and privacy compliance. While traditional malware defense systems successfully share threat signatures across boundaries, no comparable mechanism exists for natural language-based attacks on LLMs. **BinaryShield** addresses this gap by enabling organizations to share actionable threat intelligence about prompt injection attacks without violating privacy regulations or exposing sensitive user data.

The system is designed to achieve four primary objectives: (1) *Semantic Preservation*: capture the essential characteristics of malicious prompts that enable cross-service threat correlation; (2) *Privacy Guarantee*: ensure computational non-invertibility such that original prompts cannot be reconstructed from shared fingerprints hence upholding compliance with internal and government regulations (i.e. GDPR); (3) *Computational Efficiency*: enable efficient fingerprint generation and search; and (4) *Operational Compliance*: maintain strict separation of user data across compliance boundaries while enabling collaborative defense. To this end, **BinaryShield** transforms potentially malicious prompts through a series of privacy-preserving operations, ultimately producing compact binary fingerprints that can be safely shared between services while maintaining regulatory compliance. The key insight underlying our approach is that prompt injection attacks, despite surface-level variations, share semantic patterns that can be captured and compared without revealing the original content. By combining techniques from data anonymization, natural language processing, quantization and differential privacy, we create non-reversible fingerprints that preserve these essential semantic characteristics while providing privacy guarantees against reconstruction attacks.

High-Level Architecture. Figure 1 illustrates the complete **BinaryShield** system architecture. An attacker issues semantically related prompts (x, y, z) to the services of an enterprise organization that reside in separate compliance boundaries (Figure 1-❶). Each service applies their own defense mechanism ($D1, D2$, and $D3$) to incoming prompts. Service-2 flags a prompt-injection attempt (Figure 1-❷). After this step, **BinaryShield**’s fingerprinting pipeline is invoked in the service’s compliance boundary (Figure 1-❸). At this stage, the attack log is separated into two components. The first and the most critical component is private information: this contains the sensitive content of the prompt itself, holding the essential details of the attack. Although critical for accurate event correlation, this data must remain within the service’s compliance boundary to safeguard privacy due to regulatory requirements. The suspicious prompt then undergoes a series of privacy-preserving transformations to generate a non-reversible privacy fingerprint (hash) within the attacked service’s compliance boundary (Figure 1-❹). A detailed description of the privacy fingerprint generation process appears in Section 2.1. The second part consists of non-private system metadata, such as the tools used during response generation and the geographical region. Since this metadata contains no sensitive data, it can be safely shared among peer services as part of complete signature. Sharing these features enhances attack correlation by providing complementary evidence to surface relevant patterns pointing to attack source and channel, which helps reduce false positives and prioritize alerts. For instance, matching system metadata across services, such as both accessing an email tool, significantly increases the confidence in the correlation of potential attacks. Concatenating both parts forms a composite *attack fingerprint* that discloses no readable text (Figure 1-❺) This encoded hash is then securely broadcast to peer services for threat correlation (Figure 1-❻). Note that peer services (i.e., Services 1 and 3) use the exact same technique to fingerprint their local private queries and

Algorithm 1: *BinaryShield*: Privacy-Preserving Threat Intelligence Pipeline

Input: Suspicious prompt y ; system metadata m ; privacy parameter α ; set of peer services \mathcal{S}
Output: Privacy-preserving fingerprint f broadcast to \mathcal{S} ; correlated alerts at peers

```
1  $y_{redacted} \leftarrow \text{PII\_Redact}(y)$  ; // Remove all PII, replace with placeholders
2  $e \leftarrow \text{Embed}(y_{redacted})$  ; // Compute semantic embedding vector
3  $b \leftarrow []$  ; // Initialize empty binary vector
4 for  $i \leftarrow 1$  to  $d$  do
5    $b_i \leftarrow \begin{cases} 1 & \text{if } e_i > 0 \\ 0 & \text{otherwise} \end{cases}$  ;
6   Append  $b_i$  to  $b$  ;
7    $p_{keep} \leftarrow \frac{e^\alpha}{e^\alpha + 1}$  ; // Probability of keeping the true bit
8    $\tilde{b} \leftarrow []$  ; // Initialize empty privatized vector
9   for  $i \leftarrow 1$  to  $d$  do
10  | Sample  $u_i \sim \text{Uniform}(0, 1)$  ;
11  | if  $u_i < p_{keep}$  then
12  |   |  $\tilde{b}_i \leftarrow b_i$  ; // Keep the true bit
13  | else
14  |   |  $\tilde{b}_i \leftarrow 1 - b_i$  ; // Flip the bit
15  | Append  $\tilde{b}_i$  to  $\tilde{b}$  ;
16  $f \leftarrow \text{Concatenate}(\tilde{b}, m)$  ; // Combine privatized bits with non-private metadata
17 Broadcast( $f, \mathcal{S}$ ) ; // Send fingerprint to all peers
```

system metadata as used in Step ③ of Figure 1. For instance, after searching their logs, Service 1 and Service 3 independently find two and one similar attacks, respectively (Figure 1-⑥). Policy-driven response actions are then executed for each service based on the correlation results (Figure 1-⑦). *Note that there is currently no public dataset available for system metadata. Therefore, our evaluation of *BinaryShield* focuses exclusively on private information (prompt) fingerprinting. Nonetheless, including system metadata features in the overall design demonstrates the full architectural intent of *BinaryShield* and highlights additional layers of security and context.*

2.1 *BinaryShield* One-Way Fingerprint Generation Design

We consider an adversary with several capabilities: possesses white-box access, meaning they have complete knowledge of the *BinaryShield* algorithm, including the embedding models, quantization methods, and privacy parameters. The adversary’s primary objective is to reconstruct original prompts from shared fingerprint, potentially exposing sensitive user information. Our system must, therefore, prevent such reconstruction while preserving utility for effective threat detection. Based on our threat model and regulatory constraints, *BinaryShield* must satisfy several critical requirements. First, it must ensure privacy preservation by making fingerprints computationally non-invertible, thereby preventing the reconstruction of original prompts even in the case of white-box access. Second, semantic preservation remains essential; despite privacy transformations, the fingerprints must retain enough semantic information to enable the identification of similar attack patterns. Third, the system must maintain computational efficiency, capable of processing millions of queries each day with minimal latency impact. Fourth, it must offer cross-boundary compatibility, allowing fingerprints to be shared across services with varying compliance requirements without violating relevant regulations. Finally, the system must support approximate matching, enabling similarity searches that can detect related attacks despite minor variations in the input. Figure 2 and Algorithm 1 depicts the *BinaryShield* pipeline for generating privacy-preserving fingerprints (hashes) of prompt injection attacks. Below, we detail each component of the pipeline, explaining how they collectively satisfy our design requirements.

2.1.1 PII Redaction

The initial stage of the *BinaryShield* pipeline directly targets privacy risks by identifying and removing personally identifiable information (PII) that may be present in

flagged prompts. While automated defense mechanisms aim to identify malicious content, they may inadvertently flag benign prompts containing sensitive user data. A key challenge in PII redaction is removing sensitive information while preserving the semantic intent and structure of potential attacks. Our approach addresses this by detecting and redacting structured data such as social security numbers, credit card numbers, phone numbers, email addresses, as well as person names, organizations, locations, and other identifying entities. Identified PII is replaced with generic placeholders that maintain command structure, entity relationships, and linguistic patterns indicative of injection attempts. For example, "Transfer \$5000 from John Smith's account 123456789" becomes "Transfer [AMOUNT] from [PERSON]'s account [ACCOUNT]". This balance ensures the redacted text retains sufficient information for downstream processing while protecting user privacy from the earliest stage of the pipeline. By design, redaction is intended to be one-way and non-reversible: no original PII should survive beyond this step, ensuring compliance with privacy regulations before any downstream processing. While the effectiveness of redaction depends on the accuracy of underlying detection methods, our approach minimizes the risk of residual PII to the greatest extent possible. **BinaryShield** uses Microsoft's Presidio open-source library [Microsoft] for PII detection and redaction. Figure 3 reports the PII entities and their respective counts that **BinaryShield** flags in the prompt injection dataset from [Shen et al., 2024], used in **BinaryShield**'s evaluation (Section 3). However, even after PII redaction, the remaining text may still contain sensitive or revealing information that cannot be safely shared across compliance boundaries. To address this, **BinaryShield**'s pipeline generates privacy-preserving semantic fingerprints, enabling robust threat detection without exposing any underlying content.

2.1.2 Semantic Feature Extraction

Following PII redaction, **BinaryShield** must capture the semantic essence of the potentially malicious prompt in a format suitable for comparison and analysis. To this end, **BinaryShield** employs state-of-the-art transformer-based language models to generate high-dimensional embeddings that encode the semantic relationships within the text. This transformation serves as the foundation for our semantic preservation requirement. This capture the meaning and intent of the potentially malicious prompt. The embedding process transforms the redacted text into a dense vector $\mathbf{e} \in \mathbb{R}^d$, where d is the embedding dimension. The embedding space exhibits several properties that are crucial for threat detection. First, similar attack patterns tend to cluster together in the embedding space, regardless of surface-level variations. Second, the embeddings are robust to paraphrasing, so minor rewording or synonym substitution results in nearby embeddings, enabling the detection of attack variants.

Binary Quantization. While semantic embeddings effectively capture prompt meaning, they pose significant challenges for privacy-preserving threat intelligence. Dense embeddings can leak information about the original text [Walsh, Li et al., 2023, Tragoudaras et al., 2025, OWASP2025, 2025]. They also require substantial computational resources for large-scale similarity searches. Our binary quantization addresses both concerns. We transform the continuous embedding $\mathbf{e} \in \mathbb{R}^d$ into a binary vector $\mathbf{b} \in \{0, 1\}^d$ using sign-based quantization:

$$b_i = \begin{cases} 1 & \text{if } e_i > 0 \\ 0 & \text{otherwise} \end{cases}$$

where e_i is the i -th dimension of the embedding vector and b_i is the corresponding bit in the binary vector. This transformation discards magnitude information while preserving the directional (sign) information of each embedding dimension. Binary quantization provides several critical benefits: *Irreversibility*: The transformation from \mathbb{R} to $\{0, 1\}$ is many-to-one, making exact reconstruction impossible. Each bit only indicates whether the original value was positive or negative, discarding all magnitude information. *Dimensionality preservation*: Despite the dramatic reduction in information

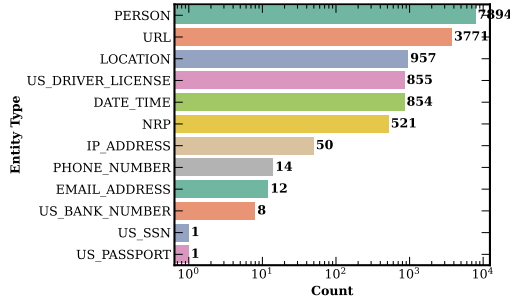


Figure 3: Distribution of PII entities in prompts flagged by **BinaryShield**. The most common entity include person names.

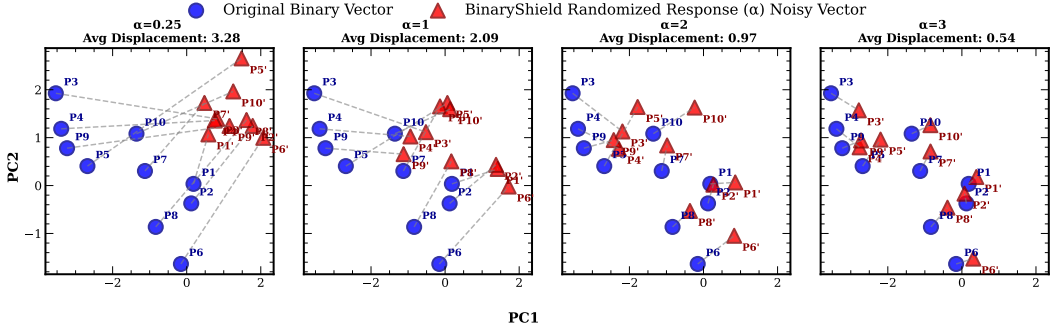


Figure 4: Impact of BinaryShield’s privacy parameter (α) on binary vector quality. As α increases, privatized vector (red triangles) move closer to original vector (blue circles), showing improved utility while maintaining differential privacy through controlled bit-flipping (i.e., $1 - p$) noise.

per dimension, the high dimensionality (d) of the binary embedding preserves the essential geometric properties needed for similarity detection. The sign of each embedding dimension collectively maintains sufficient information to distinguish between semantically similar and dissimilar prompts. *Storage efficiency*: Each dimension requires only 1 bit instead of 32 bits (float32), achieving a 32x reduction in storage requirements and even more in case of float64. Our empirical evaluation shows that binary quantization preserves semantic relationships and achieves comparable threat detection performance, while providing substantial privacy benefits (Section 3).

2.1.3 BinaryShield’s Randomized-Response Layer

While data anonymization (PII redaction) and binary quantization significantly enhances privacy, adversaries with auxiliary information might still attempt reconstruction attacks. To close this gap, the pipeline enforces *local* differential privacy (LDP) on every fingerprint by applying classical randomized response [Warner, 1965, Erlingsson et al., 2014, Wang et al., 2017] independently to each bit before the fingerprint crosses the compliance boundary. Local differential privacy is particularly attractive in cross-boundary threat-intelligence settings because the guarantee is enforced before data leave the originator’s compliance perimeter; no trusted aggregator or secure enclave is required. Even an adversary with white-box knowledge of the entire pipeline and unlimited access to all shared fingerprints cannot violate the worst-case privacy bound. Moreover, in contrast to the global-DP setting, the magnitude of noise required for LDP is independent of the dataset size, allowing BinaryShield to scale to millions of daily fingerprints without ever decreasing privacy protection. Consider a d -bit fingerprint $\mathbf{b} = (b_1, \dots, b_d) \in \{0, 1\}^d$ and let $\alpha > 0$ denote the per-bit privacy budget. Classical randomized response publishes a perturbed vector $\tilde{\mathbf{b}}$ obtained by flipping each bit independently with probability $1 - p$, where

$$p = \frac{e^\alpha}{e^\alpha + 1}$$

The mechanism releases the randomized bit.

$$\tilde{b}_i = \begin{cases} b_i & \text{with probability } p, \\ 1 - b_i & \text{with probability } 1 - p. \end{cases}$$

Randomized response inevitably perturbs the underlying signal. The expected self-distance introduced by the mechanism is

$$\mathbb{E}[\text{H}(\mathbf{b}, \tilde{\mathbf{b}})] = (1 - p)d,$$

where H denotes Hamming distance and d is the fingerprint dimensionality. The *Hamming distance* between two binary vectors $\mathbf{b}, \tilde{\mathbf{b}} \in \{0, 1\}^d$ is defined as the number of positions at which the corresponding bits differ:

$$\text{H}(\mathbf{b}, \tilde{\mathbf{b}}) = \sum_{i=1}^d \mathbb{I}[b_i \neq \tilde{b}_i]$$

where $\mathbb{I}[\cdot]$ is the indicator function, which equals 1 if its argument is true and 0 otherwise. Because p remains close to one even for moderate α , the added noise is sparse and, as we show experimentally in Section 3, preserves enough structure for accurate approximate matching while providing the formal privacy guarantees demanded by cross-service threat intelligence.

The randomization budget α serves as a control parameter governing the privacy-utility tradeoff in **BinaryShield**. When α approaches zero, the mechanism maximizes privacy protection (i.e., infinite privacy) but renders fingerprints unusable for correlation. As α increases, utility improves while maintaining privacy guarantees in a controlled manner. Figure 4 illustrates this relationship through PCA visualization of binary vectors before and after applying the Randomized Response mechanism [Warner, 1965]. At $\alpha = 0.25$, privatized vectors (red triangles) appear completely random. As α increases (reducing noise), these vectors progressively align closer to their original non-private counterparts (blue circles). Notably, even at $\alpha = 3$, a non-zero average displacement between original and privatized vectors persists, making reconstruction of the original prompt challenging. This visualization confirms that larger α values preserve more of the vector's structure while maintaining formal differential privacy guarantees through controlled bit-flipping. In practice, higher privacy budgets may be appropriate for intra-service sharing where additional security measures already exist within organizational boundaries.

2.1.4 **BinaryShield**'s Cross-Service Threat Correlation

When a service detects a potential prompt injection, it generates a fingerprint using the **BinaryShield** pipeline. For clarity, we denote the locally randomized-response fingerprint $\tilde{\mathbf{b}} \in \{0, 1\}^d$ as f when broadcasting and correlating across services (i.e., $f \approx \tilde{\mathbf{b}}$). This fingerprint is broadcast asynchronously to participating services through secure channels. Upon receiving a fingerprint, services scan their historical logs for similar instances. If matches are found, alerts are triggered and defenses can be updated proactively. To maintain privacy and compliance, only aggregate match statistics are shared, and no specific prompt content is revealed. This workflow enables rapid propagation of threat intelligence while respecting organizational boundaries. Formally, let $\mathcal{S} = \{S_1, S_2, \dots, S_N\}$ denote the set of N services, each with its own compliance boundary. Each service S_i maintains a log of previously observed fingerprints $\mathcal{F}_i = \{f_i^{(1)}, f_i^{(2)}, \dots, f_i^{(M_i)}\}$, where $f_i^{(m)} \in \{0, 1\}^d$ is a d -dimensional binary fingerprint. Suppose service S_q detects a suspicious prompt and generates a fingerprint $f_q \in \{0, 1\}^d$ using the **BinaryShield** pipeline. This fingerprint is securely broadcast to all other services S_j ($j \neq q$). Each recipient service S_j performs the following search:

$$\mathcal{M}_j(f_q) = \left\{ f_j^{(m)} \in \mathcal{F}_j \mid H(f_q, f_j^{(m)}) \leq \tau \right\}$$

where $\mathcal{M}_j(f_q)$ is the set of fingerprints belonging to service S_j (i.e., fingerprints in \mathcal{F}_j) that match f_q within a Hamming distance threshold τ , and $H(\cdot, \cdot)$ is the Hamming distance as previously defined. This protocol enables rapid, privacy-preserving propagation of threat intelligence across all N services. This protocol generalizes to any number of services. For example, if Service 2 (S_2) generates a fingerprint f_2 , it broadcasts f_2 to Services 1 and 3 (S_1, S_3), which independently search their logs for similar fingerprints. If S_1 finds two matches and S_3 finds one, these services take action based on their policy and only the counts are reported back, enabling rapid, privacy-preserving propagation of threat intelligence across organizational boundaries.

Overall, when a match is found below a calibrated threshold, the service can take protective actions such as updating classifier parameters, flagging suspicious activity, or blocking potential attacks. Services can subscribe to threat intelligence feeds from peer services, automatically incorporating new attack patterns into their defense mechanisms.

Summary. **BinaryShield** offers a scalable and privacy-preserving solution for sharing prompt injection threat intelligence across organizational and compliance boundaries. By combining PII redaction, semantic embedding, binary quantization, and differential privacy, the system achieves strong privacy protections without sacrificing detection performance or scalability. The modular architecture allows for privacy parameters to be tuned to specific requirements, while efficient processing supports production-scale deployments. As large language model adoption expands,

BinaryShield establishes a foundation for collaborative and adaptive defenses against evolving prompt injection attacks.

3 Evaluation

We conduct a comprehensive evaluation of BinaryShield to assess its effectiveness in privacy-preserving threat intelligence sharing for prompt injection attacks. Our evaluation addresses key research questions across diverse, systematically generated attack variants. BinaryShield’s evaluation is structured around the following research questions:

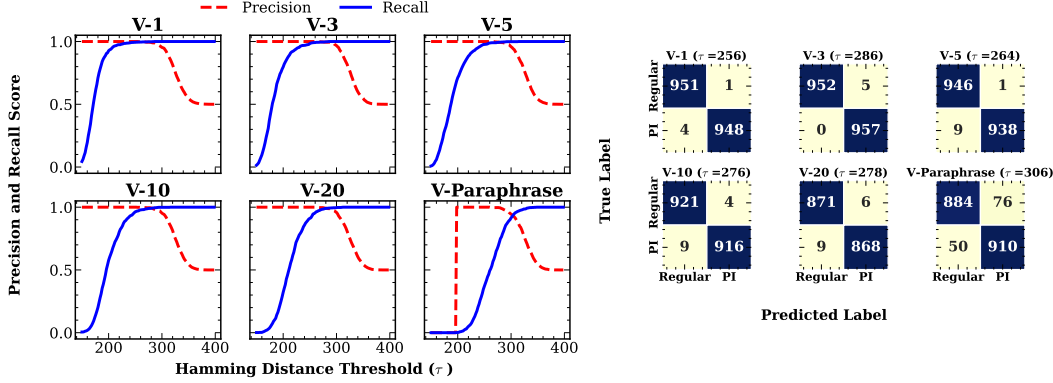
- **RQ1 (Detection Effectiveness).** How accurately does BinaryShield detect prompt injection attacks across systematically generated adversarial variants, from simple word substitutions to comprehensive semantic paraphrasing, compared to the SimHash baseline?
- **RQ2 (Privacy-Utility Trade-off).** What is the quantitative relationship between BinaryShield’s randomized response mechanism (α) and threat detection utility?
- **RQ3 (Noise Calibration & Predictability).** Does the empirical self-Hamming distortion introduced by randomized response match the theoretical $(1 - p)d$ curve across α , letting us confidently choose a privacy setting?
- **RQ4 (Scalability).** Does BinaryShield maintain consistent detection accuracy as corpus size scales from thousands to hundreds of thousands of entries, reflecting realistic enterprise deployment scenarios where malicious prompts are sparse within benign prompts?
- **RQ5 (Computational Efficiency).** What are the computational and storage efficiency gains of BinaryShield’s binary fingerprints compared to dense embeddings, and do these improvements enable practical real-time threat correlation at enterprise scale?

3.1 Evaluation Settings

3.1.1 Datasets

We evaluate BinaryShield using the recent prompt injection dataset from [Shen et al., 2024], which contains real-world attack and benign prompts. From this, we construct a comprehensive evaluation set simulating adversarial scenarios, enabling controlled and realistic assessment of threat intelligence in LLM services.

Given the inherent challenge of obtaining large-scale labeled datasets of semantically similar prompt injection variants, we develop a systematic methodology for generating controlled attack modifications to validate threat intelligence. Our synthetic data generation process creates two primary types of variants: *Word-Flipping Variants*: For each adversarial prompt, we randomly select x words (where $x \in \{1, 3, 5, 10, 20\}$) longer than four characters and replace them with semantically equivalent synonyms using GPT-4o. This simulates subtle adversarial modifications that maintain attack intent while altering surface-level tokens. The language model is guided using the structured prompt: *"Understand this adversarial prompt: <original prompt>. Now generate synonyms for the following words: <words to change>. Return the JSON with the field 'words_changes_to' containing the synonyms in order."* *Paraphrase Variants*: We generate comprehensive paraphrased versions of prompts using GPT-4o while preserving the underlying attack intent and malicious purpose. The generation prompt instructs the model: *"Paraphrase the following adversarial prompt while maintaining the attack intent and purpose. Original prompt: <original prompt>. Return the JSON with the field 'generated_response'."* *Benign Pairs*: Benign prompts are systematically paired such that each pair consists of two semantically unrelated prompts, ensuring they serve as appropriate negative examples for similarity detection algorithms (e.g., SimHash and BinaryShield). The resulting dataset undergoes rigorous filtering to ensure quality and consistency (e.g., remove duplicates, empty prompts). The final dataset is balanced with equal numbers of attack and benign pairs, with attack pairs labeled as 1 and benign pairs labeled as 0. This balanced approach ensures unbiased evaluation across both positive and negative cases. Our synthetic generation methodology enables systematic evaluation across varying levels of attack sophistication, from minimal single-word modifications to comprehensive paraphrasing that significantly alters surface structure while preserving malicious intent. This controlled approach allows us to assess algorithm robustness across the spectrum of adversarial modifications likely encountered in real-world deployment scenarios.



(a) Precision-recall curves across attack variants. (b) Confusion matrices at optimal thresholds.

Figure 5: **BinaryShield** performance analysis across attack variants with $\alpha = 2.0$. (a) Precision-recall curves demonstrate consistent performance across variants. (b) Confusion matrices at optimal Hamming distance thresholds show TP, TN, FP, and FN counts, indicating strong detection capabilities even under complex paraphrasing attacks. Note that **PI** in the confusion matrices stands for *Prompt Injection* and is used to distinguish between attack and benign prompts.

3.1.2 Baseline

Our evaluation compares two primary approaches for prompt similarity detection **BinaryShield** and SimHash. **BinaryShield** utilizes ModernBert for semantic feature extraction, followed by sign-based binary quantization and randomized response for local differential privacy. We also evaluate it with OpenAI embedding model to demonstrate the flexibility of **BinaryShield** in supporting both open source and closed source models. SimHash is a widely-adopted locality-sensitive hashing algorithm that serves as our primary baseline. SimHash generates compact binary fingerprints and has been extensively used for near-duplicate detection in large-scale text corpora [Manku et al., 2007].

3.1.3 Evaluation Metrics

We employ a comprehensive set of metrics to assess both detection performance and privacy-utility tradeoffs. For detection performance, we use precision, recall, accuracy, and F1-score across varying similarity thresholds to evaluate attack detection accuracy. Threshold analysis is performed using precision-recall curves to identify the optimal threshold for Hamming distance and to understand how performance is affected by threshold selection, as discussed in [Manku et al., 2007]. We also include confusion matrices for detailed analysis of true positives (TP), false positives (FP), true negatives (TN), and false negatives (FN) at optimal thresholds.

3.2 BinaryShield Comparison with Baseline

To provide a rigorous performance analysis, we systematically compare **BinaryShield** against SimHash, a widely used locality-sensitive semantic hashing method [Manku et al., 2007]. Both algorithms generate binary fingerprints and use Hamming distance for similarity measurement, making them directly comparable. This baseline is chosen to evaluate not only detection performance but also the privacy-preserving capabilities essential for cross-boundary threat intelligence sharing as SimHash also generates non-reversible binary fingerprints.

For this *evaluation*, we configure **BinaryShield** with a differential privacy parameter of $\alpha = 2.0$, which provides meaningful privacy protection while maintaining strong detection performance. We note that **BinaryShield** with ModernBert generates 768-dimensional binary vector while SimHash produces 64-dimensional vector.

Our comparative analysis encompasses six distinct attack variants: minimal single-word modifications (V-1), progressive word changes (V-5, V-20) and extensive modifications in paraphrasing scenarios (V-Paraphrase) that fundamentally restructure prompts while preserving malicious intent. This progression allows us to assess how each method's

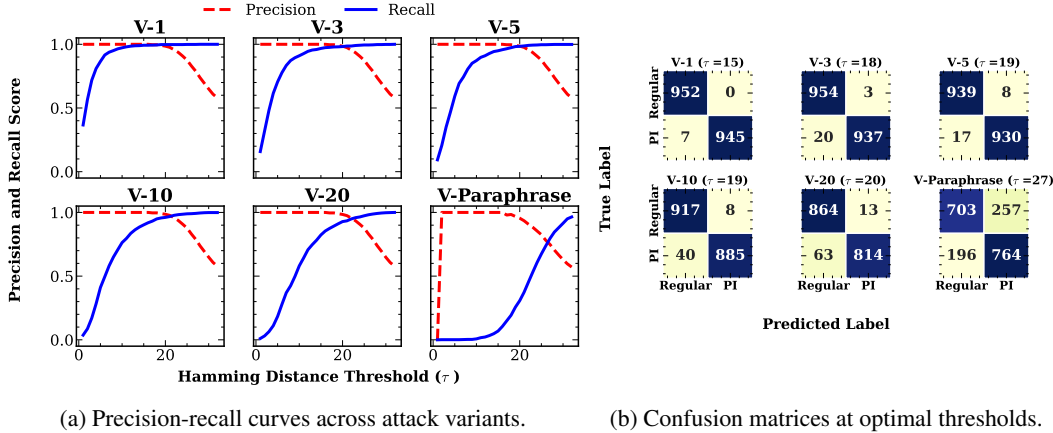


Figure 6: **SimHash** baseline performance analysis across attack variants. Confusion matrices reveal growing FP and FN, particularly for paraphrasing scenarios where token-based similarity detection struggles.

performance degrades as attack sophistication increases during threat correlation. Figure 5 and Figure 6 present comprehensive performance analysis through precision-recall curves (subfigures -a) and confusion matrices at optimal operating points (subfigures -b). For minimal attack modifications (V-1 to V-10), both algorithms demonstrate exceptional detection capabilities with near-perfect performance (Figure 7). At optimal thresholds, both methods achieve optimal F1-scores (Figure 7), establishing a strong baseline for more complex evaluations. For instance, in the V-10 scenario, SimHash produces 8 false positives and 40 false negatives at Hamming distance threshold (τ) 19 (Figure 6), while BinaryShield generates only 4 false positives at threshold 276 (Figure 5).

As attack complexity increases to extensive word modifications (V-20), performance differences begin to emerge. BinaryShield maintains robust performance with an F1-score of 0.99 (precision: 0.99, recall: 0.98), while SimHash experiences measurable degradation to an F1-score of 0.96 (precision: 0.98, recall: 0.93). The 3.3 percentage point gap starts to illustrate BinaryShield’s superior stability as lexical modifications increase.

The most challenging scenario involves comprehensive paraphrasing attacks (V-Paraphrase), where prompts undergo fundamental restructuring while preserving malicious intent. Here, the performance differential becomes most pronounced: BinaryShield achieves an F1-score of 0.94 (precision: 0.92, recall: 0.95), while SimHash degrades significantly to an F1-score of 0.77 (precision: 0.75, recall: 0.80). This 17 percentage point gap in F1 score demonstrates BinaryShield’s fundamental advantage in threat intelligence that transcends surface-level linguistic variations.

Additionally, examining *confusion matrices* at optimal thresholds, provides additional insights into error patterns in Figures 5b and 6b. BinaryShield demonstrates consistent performance as compared to SimHash. SimHash shows increasing error variability as attack complexity increases, struggling particularly to distinguish between semantically similar malicious content and unrelated benign prompts in paraphrasing scenarios.

Our empirical results demonstrate that BinaryShield provides superior robustness for prompt injection threat correlation compared to SimHash, with advantages becoming most pronounced for

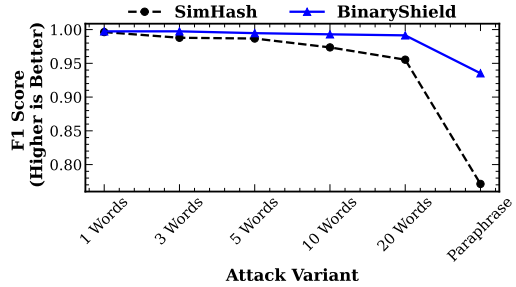


Figure 7: F1-score comparison between BinaryShield and SimHash across attack variants. BinaryShield consistently outperforms SimHash, particularly in complex paraphrasing scenarios, demonstrating superior robustness to semantic modifications.

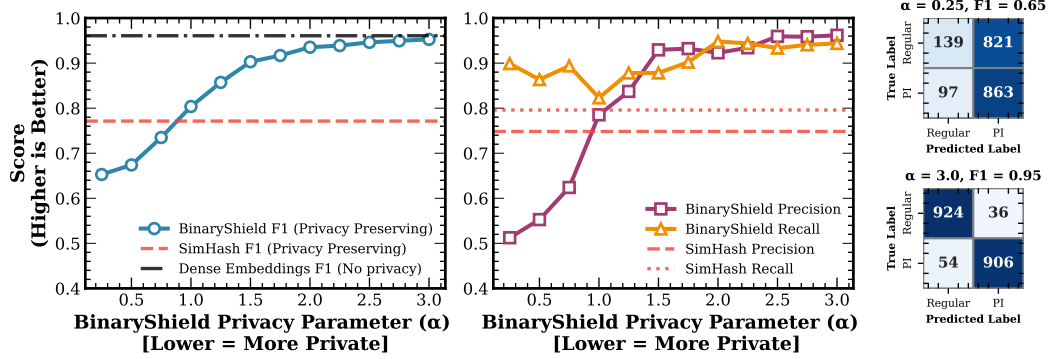


Figure 8: Privacy-utility trade-off for paraphrased prompt injection detection. (Left) BinaryShield F1 rises smoothly with privacy budget α , dominating SimHash (privacy-preserving baseline) across most of the spectrum and approaching non-private dense embeddings. (Center) Precision lags recall at high noise, then rapidly converges after $\alpha \approx 1$ as false positives collapse. Horizontal dashed lines: SimHash precision/recall. (Right) Confusion matrices at extreme settings: severe noise ($\alpha = 0.25$) induces many false positives; higher α (3) sharply improves precision.

sophisticated attacks that represent complicated adversarial scenarios. The 17 percentage point F1-score gap in paraphrasing attacks, the most challenging and operationally relevant scenario, validates the effectiveness of BinaryShield over semantic hashing technique like SimHash. These performance improvements are achieved while simultaneously providing privacy guarantees essential for cross-boundary threat intelligence sharing. The superior performance on complex attacks is particularly significant, as sophisticated paraphrasing and extensive modification represent the most realistic attack patterns likely to be encountered in production environments where adversaries actively attempt to evade detection systems.

Summary. BinaryShield consistently outperforms SimHash in prompt injection threat correlation, especially under complex paraphrasing attacks, achieving an F1-score of 0.94 compared to SimHash’s 0.77. These results highlight BinaryShield’s superior robustness with enabling privacy, making it highly effective for cross-boundary threat intelligence sharing.

3.2.1 Empirical Analysis of Randomized Response Impact

We quantify the impact of randomized response mechanism [Warner, 1965] noise on detection utility by sweeping the per-bit privacy budget $\alpha \in [0.25, 3.0]$ (Algorithm 1, Step 4) on the most challenging paraphrase attack variant. For each α , a bit in the 768-dimensional binary embedding is kept with probability $p = \frac{e^\alpha}{e^\alpha + 1}$ and flipped otherwise, yielding an expected self-Hamming distortion $(1 - p)d$, where d is the fingerprint dimension (here, $d = 768$). At $\alpha = 0.25$, $p = 0.562$ and the mechanism flips $\approx 0.438 \times 768 \approx 336$ bits (i.e., the whole binary vector is approximately completely randomized). As shown in the top-right confusion matrix of Figure 8, at this extreme privacy setting there are 821 false positives and 97 false negatives, resulting in an F1-score of only 0.65. Such high noise levels provide maximal privacy but render the binary fingerprints nearly random (Figure 9), offering little practical utility for threat detection.

Figure 8 shows that utility improves smoothly and monotonically with larger α as noise shrinks. At $\alpha = 1.0$ precision increases to 0.79 with high recall of 0.82. The inflection region $\alpha \in [1.25, 1.75]$ marks the transition where precision catches up to recall: by $\alpha = 1.5$ BinaryShield attains F1=0.90, already exceeding SimHash’s paraphrase F1 (0.77) by +13 points while providing privacy that is absent in dense cosine embeddings. From $\alpha = 2.5$ onward the F1 curve is close to the dense embeddings while still providing privacy as bit flipping probability is not zero (Figure 9). The confusion matrices at the privacy extremes (Figure 8, right) illustrate this shift: moving from $\alpha = 0.25$ to 3.0 reduces false positives 22.8× (821→36) and false negatives (97→54), yielding an approximately 30-point F1 gain (0.65→0.95). This predictable performance curve lets operators easily adjust α to meet privacy requirements, estimate detection accuracy, and securely share threat intelligence without revealing raw prompts or embeddings.

Randomized Response and Hamming Distance. To empirically validate **BinaryShield**’s privacy model, we conducted a controlled experiment measuring the actual Hamming distance introduced by the **BinaryShield**’s randomized response mechanism.

To this end, for 500 prompts from our evaluation dataset, **BinaryShield** generated 768-dimensional binary fingerprints and applied its differential privacy transformation by varying α values from 0.2 to 3.4. For each configuration, we computed the Hamming distance between original and noise-perturbed fingerprints, comparing observed distances against the theoretical expectation $(1 - p)d$. As a baseline reference, we generated 1,000 pairs of independent random binary vectors to establish the average distance for completely uncorrelated binary vectors. The mean Hamming distance for these independent vectors is 384.44 ± 13.65 , which serves as a baseline for comparison. Figure 9 demonstrates that our theoretical model precisely predicts the observed self-Hamming distortion across all privacy levels confirming **BinaryShield**’s alignment with theory. At $\alpha = 0.2$, **BinaryShield**’s perturbed binary fingerprint reaches a Hamming distance of 346 ± 13.41 , nearly matching the random baseline. This results in lower F1 scores at small α (Figure 8).

As α increases, the Hamming distance decreases to 206.45 ± 13.08 at $\alpha = 1.0$. This decay directly correlates with the smooth utility recovery in Figure 8. The tight correspondence between theoretical predictions and observed measurements validates that **BinaryShield**’s privacy mechanism operates exactly as designed, providing operators with precise control over the privacy-utility trade-off through a single, well-characterized parameter α . Another noticeable observation is that even at higher α values, as shown in Figure 9, the Hamming distance remains nonzero. This indicates that **BinaryShield** continues to provide privacy protection, since the nonzero Hamming distance ensures privacy is maintained, even as its utility approaches that of dense embeddings (Figure 8 and 9). In contrast, dense embeddings offer no privacy at all, so even a nonzero Hamming distance (i.e., some privacy) is fundamentally better than nothing, ensuring that sensitive information is not directly exposed.

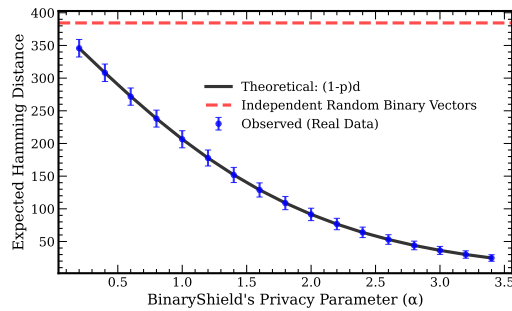


Figure 9: Calibration of randomized-response noise. Empirical mean Hamming distances (blue points, $n = 500$ each) between original and privatized 768-bit fingerprints tightly follow the theoretical curve $(1 - p)d$ (solid black) across privacy budgets α . The dashed red line shows the mean distance between independent random binary vectors (384), illustrating how increasing α moves **BinaryShield** smoothly from near-randomization to low-distortion states.

Summary. **BinaryShield** exhibits the fundamental differential privacy trade-off: low α (strong privacy) yields near-random fingerprints, whereas increasing α (meaningful privacy) produces a smooth, monotonic F1 rise that quickly approaches non-private baseline performance.

3.3 Real-World Deployment Analysis

While earlier sections validate **BinaryShield**’s superior performance as compared to privacy preserving baseline (SimHash), we now turn to evaluating **BinaryShield**’s effectiveness in realistic cross-service threat intelligence scenarios. Specifically, it must be shown that privacy-preserving correlation remains effective when (i) malicious prompts are sparse relative to benign traffic and (ii) corpus size scales by an order of magnitude (iii) Privacy-utility trade-off is maintained, i.e., the accuracy gap between **BinaryShield** and non-private dense embeddings remains bounded, and (iv) efficiency is maintained in terms of computational and storage overhead.

We study this setting using hybrid corpora that interleave a (fixed) malicious prompt injection (V-Paraphrase) with large volumes of real user interactions from WildChat [Zhao et al., 2024], thereby emulating an enterprise log in which only a small fraction of entries are prompt injection attacks.

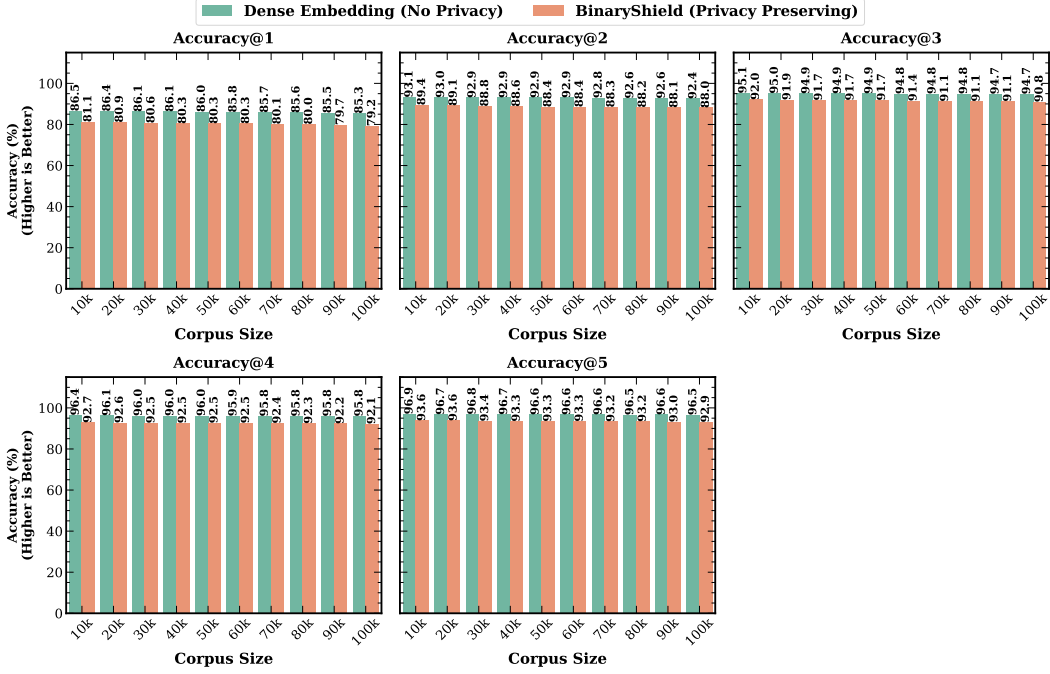


Figure 10: Scalability of privacy-preserving threat correlation. Accuracy@k for BinaryShield vs non-private dense embeddings baseline across hybrid corpora (10K-100K). Accuracy remains flat with scale; BinaryShield retains 93% of baseline Accuracy@1 while providing privacy.

3.3.1 Large-Scale Threat Intelligence Scalability

The goal is to quantify how BinaryShield’s privacy-preserving fingerprint correlation accuracy behaves as the total corpus grows from 10K to 100K entries, and characterize the accuracy gap relative to a non-private dense embedding baseline. In this experiment, BinaryShield uses OpenAI’s text-embedding-3-large to generate dense embeddings. For each target corpus size $C \in \{10K, 20K, \dots, 100K\}$, we construct a hybrid dataset by injecting a fixed malicious prompt set into $C - M$ benign WildChat prompts (where M is the number of distinct attack prompts). Each malicious prompt is issued as a query; success is recorded if its exact counterpart (or semantically identical variant, depending on k) appears within the top- k candidates when ranked by Hamming distance over BinaryShield’s fingerprints, or cosine similarity for the dense baseline. We fix the local differential privacy parameter at $\alpha = 2$ (different α values are also evaluated in Section 3.3.2).

Figure 10 shows the results of threat intelligence scalability analysis, with the X-axis showing corpus sizes (10K to 100K) and the Y-axis representing retrieval accuracy. Accuracy@ k represents the percentage of queries for which the correct malicious prompt is returned in the first k -results. Accuracy@1 for the dense baseline declines modestly by only 1.2% points across a 10 \times increase in corpus size (86.5% \rightarrow 85.3%). BinaryShield shows a similarly shallow decline (81.1% \rightarrow 79.2%; 1.9% points). This indicates that neither binary quantization nor randomized response mechanism introduces scale-sensitive degradation.

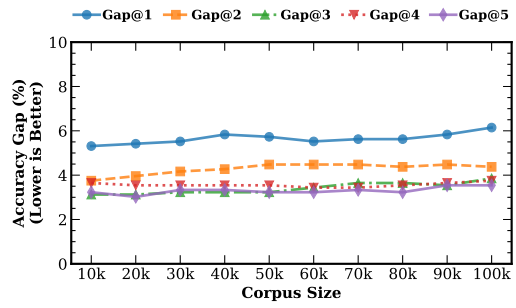


Figure 11: Accuracy@k gap (Dense Embeddings - BinaryShield) across corpus sizes. Rapid narrowing for higher k demonstrate that binary quantization plus local DP introduce a constant, not compounding, utility cost.

Furthermore, Figure 11 shows that the Accuracy@ k *gaps* between BinaryShield and the dense baseline with X-axis showing corpus sizes (10K to 100K) and Y-axis showing the gap at different top- k accuracy. The gap remains tightly bounded: it ranges from 5.31 to 6.15 percentage points (mean 5.66% points) at $k = 1$, indicating that BinaryShield retains over 93% of the dense baseline’s accuracy even under tight local differential privacy constraints. Crucially, the gap does *not* significantly widen with corpus size. Furthermore, increasing k rapidly closes the gap, as shown in Figure 10 and Figure 11. For instance at 100K entries, BinaryShield achieves 79.2% Accuracy@1, 90.8% Accuracy@3, and 92.9% Accuracy@5. On the same 100K corpus, the dense embeddings achieve 85.3% Accuracy@1, 94.7% Accuracy@3, and 96.5% Accuracy@5. The gap at $k = 5$ is only 3.6% points, indicating that BinaryShield’s with privacy feature reaches close to the *non-private* baseline of dense embeddings. This confirms that the semantic signal preserved after (i) sign-only quantization and (ii) per-bit randomized response still remains sufficiently rich for practical threat correlation. For every corpus size, BinaryShield’s incremental gains from $k = 1$ to $k = 2$ average roughly +8 percentage points (Figure 10). This reflects that most residual misses at $k = 1$ are near-boundary semantic neighbors retrievable with minimal expansion. Subsequent marginal gains ($k > 2$) diminish smoothly. Figure 11 shows the gap curves monotonically compress as k increases. The gap is attributable to two irreversible transformations: (a) many-to-one sign mapping (loss of magnitude information) and (b) randomized response bit flips calibrated by $\alpha = 2$. That the gap does not drift upward with scale empirically supports that these transformations in BinaryShield behave as *scale-neutral perturbations* rather than compounding sources of semantic erosion. In an operational setting where an analyst (or automated response engine) can examine the top 3–5 correlated candidates, BinaryShield delivers privacy-preserving threat intelligence with accuracy comparable to a fully non-private dense embedding pipeline. This constitutes a strong utility guarantee under stringent local privacy constraints and validates BinaryShield’s suitability for multi-service deployment where corpus sizes routinely exceed tens of thousands of daily log entries.

Summary. BinaryShield achieves over 93% accuracy of dense embeddings (*non-private baseline*) and remains scalable in practical deployment settings with randomized response mechanism, demonstrating robust privacy-preserving threat correlation at enterprise scale.

3.3.2 BinaryShield’s Privacy Parameter Performance at Scale

The relationship between privacy protection and threat detection utility at scale represents a fundamental tension in the cross-boundary threat intelligence system. Similar to Section 3.2.1, to characterize this trade-off precisely, we evaluate BinaryShield’s performance across a spectrum of privacy budgets (α) on a fixed 50K-entry hybrid corpus containing both malicious prompts and benign WildChat interactions (Section 3.3.1). The privacy parameter α directly controls the randomized response mechanism through the bit preservation probability $p = e^\alpha / (e^\alpha + 1)$, with the corresponding bit flip probability being $1 - p$. Smaller α values provide stronger privacy guarantees by increasing the probability of bit flips in the binary fingerprint, while larger values preserve more semantic information at the cost of reduced privacy protection.

Our experimental results, visualized in Figure 12, reveal a sharp phase transition in detection accuracy as the privacy budget increases from highly restrictive to meaningful protective settings. The X-axis represents the privacy parameter α , while the Y-axis shows correlation accuracy (Accuracy@1 and Accuracy@5) for both BinaryShield and the *non-private* dense embedding baseline.

At extreme privacy levels ($\alpha = 0.1$), the bit flip probability reaches 0.475, meaning nearly half of all bits are randomly inverted, effectively reducing fingerprints to near-random noise. Consequently,

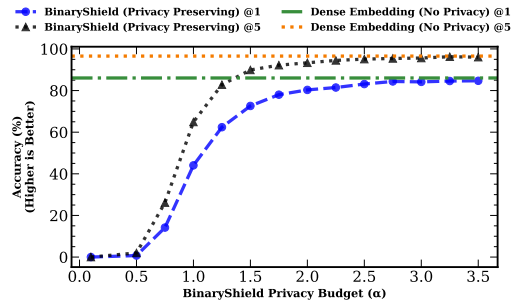


Figure 12: Privacy-utility trade-off for BinaryShield across α values on 50K hybrid corpus. Accuracy@1 (blue line) and Accuracy@5 (dotted black line) show phase transition behavior as privacy budget increases. The non-private dense embedding baseline is shown as horizontal green and orange lines at 86.04% (Accuracy@1) and 96.56% (Accuracy@5) respectively.

15

Accuracy@1 drops to 0%, rendering threat correlation impossible. This represents the theoretical limit where maximal privacy completely eliminates utility. As we relax the privacy constraint the bit flip probability decreases. With $\alpha = 0.75$ (bit flip probability 0.32), Accuracy@1 rises to 14.17% and Accuracy@5 to 26.15%, marking the onset of effective threat detection. At $\alpha = 1.0$ BinaryShield reaches 44.06% Accuracy@1 and 64.90% Accuracy@5. While this is roughly half the non-private baseline (86.04% and 96.56%), it shows that meaningful threat correlation is feasible even under strong privacy constraints. Between $\alpha = 1.0$ and $\alpha = 2.0$, accuracy improves smoothly with meaningful privacy and utility tradeoff. At $\alpha = 1.25$, Accuracy@1 reaches 62.40% and Accuracy@5 82.81%. At $\alpha = 1.5$, Accuracy@1 is 72.60% and Accuracy@5 is 89.90%, retaining 84.4% of baseline Accuracy@1.

The results show a smooth transition in the privacy-utility trade-off, especially between $\alpha = 0.75$ and $\alpha = 2.0$. For significantly high-privacy needs, $\alpha = 1.5$ gives strong privacy. Since organizations have already strict security policies, for internal sharing, relaxing privacy to $\alpha = 2.0\text{--}2.5$ yields near-optimal utility with *realistic* meaningful privacy protection. Overall, BinaryShield potentially can operate in a wide range of privacy-utility trade-offs.

Summary. BinaryShield empowers organizations to balance privacy and utility as needed, consistently delivering strong accuracy and realistic privacy protection. The organizations can flexibly tune the privacy-utility trade-off based on their operational needs, regulatory requirements, and threat detection scenarios.

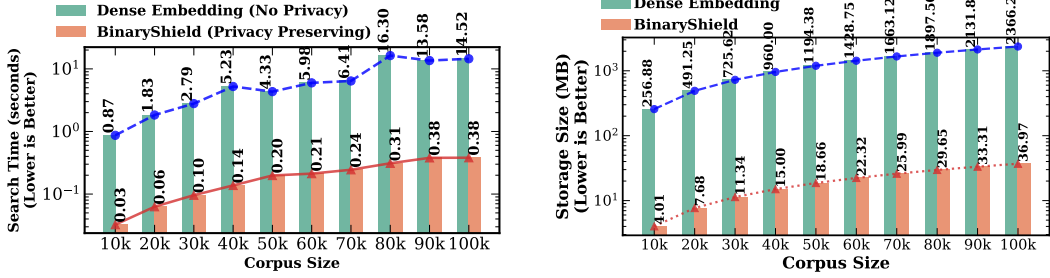
3.3.3 BinaryShield Computational and Storage Efficiency Analysis

The operational viability of any threat intelligence system fundamentally depends on its ability to process vast quantities of data with minimal latency and storage overhead. Historical lessons from traditional cybersecurity infrastructure underscore this requirement. One of the major reason that signature-based ecosystems (antivirus, IDS) scaled is because compact hashes (e.g., MD5, fuzzy-hash families). Similarly, modern LLM services face an even more daunting challenge, processing billions of queries daily across distributed infrastructure. For BinaryShield to enable practical cross-boundary threat intelligence, it must achieve orders-of-magnitude improvements in both computational speed and storage efficiency compared to *non-private* dense embeddings. *Every extra byte per fingerprint multiplies into material storage cost, and every millisecond of per-fingerprint scan latency stretches incident response time.*

Figure 13a reveals the stark *computational advantages* of BinaryShield’s binary fingerprints over dense embeddings. At a corpus size of 10K entries, dense embeddings require 0.87 seconds for similarity search of 968 prompt injections, while BinaryShield completes the same operation in just 0.032 seconds, a 26.7x speedup. This performance gap widens dramatically as corpus size increases. At 100K entries, dense embeddings demand 14.52 seconds, rendering real-time threat correlation infeasible for high-volume services. In contrast, BinaryShield maintains sub-second performance at 0.38 seconds, achieving a 38.1x speedup. The computational efficiency stems from the fundamental difference in similarity computation. Dense embeddings require floating-point dot products or cosine similarity calculations across thousands of dimensions, operations that scale poorly even with optimized linear algebra libraries. BinaryShield’s binary fingerprints enable Hamming distance computation through simple XOR operations.

The storage requirements present an equally compelling case for BinaryShield’s architecture, as illustrated in Figure 13b. Dense embeddings consume 256.88 MB for 10K entries, growing linearly to 2,366.25 MB at 100K entries. This represents a substantial infrastructure burden when organizations must maintain threat intelligence databases spanning billions of historical queries across multiple compliance boundaries. BinaryShield reduces storage requirements by a factor of 64, requiring only 4.01 MB for 10K entries and 36.97 MB for 100K entries. This 64x reduction directly translates from the binary quantization process, where each embedding dimension is compressed from a floating-point value to a single bit, followed by the addition of noise through randomized response that preserves the binary nature.

The practical implications of these efficiency gains extend beyond raw performance metrics (Section 3.2 and 3.3.1). Consider an organization processing 100 million queries daily across ten compliance boundaries. With dense embeddings, maintaining a rolling 30-day threat intelligence window would require approximately 7.1 TB of storage per boundary and dedicated GPU clusters for



(a) Search time comparison between non-private dense embeddings and **BinaryShield** across corpus sizes. Note the logarithmic scale on the Y-axis. Dense embeddings exhibit super-linear growth reaching 16.3 seconds at 80K entries, while **BinaryShield** maintains sub-second performance throughout, demonstrating its suitability for real-time threat correlation at enterprise scale.

(b) Storage size comparison demonstrating **BinaryShield**'s 64x reduction compared to dense embeddings. Dense embeddings scale from 256.88 MB at 10K entries to 2,366.25 MB at 100K entries, while **BinaryShield** requires only 4.01 MB to 36.97 MB respectively, enabling cost-effective long-term threat intelligence retention.

Figure 13: Computational and storage efficiency analysis of **BinaryShield** versus dense embeddings.

similarity search making it near to impractical choice. **BinaryShield** reduces this to 111 GB per boundary, fitting comfortably in memory on commodity servers while enabling CPU-based similarity search at wire speed. This efficiency democratizes threat intelligence capabilities, allowing even resource-constrained services to participate in collaborative defense without significant infrastructure investment.

Furthermore, the computational efficiency enables new operational capabilities previously infeasible with dense embeddings. Security teams can now perform retrospective threat hunting across months of historical data in minutes rather than hours. The reduced storage footprint also facilitates comprehensive threat intelligence archival, enabling long-term trend analysis and attribution of persistent attack campaigns that evolve over extended periods.

Summary. **BinaryShield**'s computational and storage efficiency fundamentally transforms cross-boundary threat intelligence economics. By reducing search latency up to 38x and storage requirements up to 64x while maintaining 93% of non-private baseline top-1 accuracy with privacy, **BinaryShield** enables enterprise-scale threat correlation. This positions **BinaryShield** as a practical foundation for collaborative threat intelligence systems against prompt injection attacks that respect regulatory boundaries while enabling effective cross-service intelligence sharing.

4 Related Work and Discussion

Prompt injection attacks pose significant risks to LLMs by embedding covert instructions within benign-looking input data to manipulate model outputs. A number of recent studies have explored both the attack methods and potential defenses against these vulnerabilities.

4.1 Attacks

Several works have focused on systematically characterizing these attacks. For instance, Greshake et al. [2023] demonstrate how hidden instructions can be inserted into external content to trigger unexpected and potentially harmful model behavior. A detailed taxonomy is provided to map out potential vulnerabilities in systems that incorporate untrusted external content. Other works [Wei et al., 2023, Zou et al., 2023, Zhang et al., 2024, Deng et al., 2024a, Huang et al., 2024, Liu et al., 2024, Shen et al., 2024, Deng et al., 2024b, Chao et al., 2025] further contribute to our understanding by exploring a variety of prompt injection scenarios. In addition, Yang et al. [2024] propose SOS, a training-time “soft prompt” attack that implants backdoors into open-source LLMs. The LLM behaves normally, until a trigger token activates malicious behaviors like jailbreaks, prompt stealing,

or output manipulation. In contrast, Russinovich et al. [2025] introduce *Crescendo*, an inference-time jailbreak attack that unfolds over multiple dialogue turns. Unlike single-turn prompt injections, *Crescendo* begins with a benign query and gradually steering the model toward generating restricted content, thereby incrementally eroding the model’s safety alignment. Supporting this observation, Bullwinkel et al. [2025] performs an in-depth analysis of such multi-turn jailbreak attacks and show why defenses designed for single-turn interactions, like circuit breakers [Zou et al., 2024], may be insufficient. By examining internal model representations, Bullwinkel et al. [2025] shows that multi-turn prompts can gradually reframe harmful outputs as safe, effectively evading safeguards designed for single-turn interactions. Yi et al. [2025] propose *BIPIA*, a framework to evaluate indirect prompt injection attacks. Their work systematically assesses the risks posed by malicious instructions embedded in third-party content and introduces two defense paradigms: one based on prompt engineering and in-context strategies in a black-box setting, and another using adversarial training with special tokens in a white-box setting. Finally, Abdelnabi et al. [2025b] introduces a realistic testbed for indirect prompt injection attacks targeting an LLM-based email assistant. In this challenge, attackers craft emails that must evade multiple defenses, such spotlighting, classifier-based filters (Prompt Shield), LLM-as-Judge, and TaskTracker to trigger unauthorized tool calls (e.g., sending an email). Conducted as a black-box competition study highlights the challenges of distinguishing injected malicious instructions from benign data. Collectively, these studies provide a comprehensive overview of the diverse strategies employed to exploit prompt injection attacks, underscoring the ongoing need for robust security measures in LLM-integrated applications and services.

4.2 Attack Defenses

Recent work proposes a variety of defense strategies against prompt injection attacks. These approaches differ in their methods and operating settings, ranging from inference-time countermeasures to white-box techniques and architectural safeguards.

Yuan et al. [2024] propose *RigorLLM* framework that enhances content moderation by (a) enriching training data with diverse adversarial examples using constrained energy-based generation, (b) appending an optimized “safe suffix” to incoming prompts to mitigate adversarial modifications, and (c) fusing predictions from a robust KNN classifier and a fine-tuned LLM to reliably detect harmful content. Hines et al. [2024] build on the work of Yi et al. [2025]¹ to address indirect prompt injection attacks by proposing a defense strategy based on *spotlighting*. This approach comprises a set of prompt-engineering techniques that transparently indicate the provenance of each input segment to assist LLM while generating response. The methods operate exclusively at inference time and do not require access to the model’s internals, making them readily applicable to API-based models. Debenedetti et al. [2025] propose *CaMeL*, a defense mechanism that explicitly detects and prevents prompt injection attacks by designing a secure execution layer around LLM operations. The work sits at the intersection of generative AI and software security, bringing established principles from the latter to protect emerging systems. Abdelnabi et al. [2025a] proposes *TaskTracker*, white-box defense, that centers on tracking the model’s internal activations before and after processing external text. By calculating the change (or “delta”) between these activations, the system can flag when the model’s task representation has been altered by injected instructions. This drift is used as a proxy to signal potential prompt injections. Liu et al. [2025] introduces *DataSentinel* that detects prompt injection attacks by fine-tuning a language model with a game-theoretic mini-max optimization. It uses a detection instruction embedding a secret key to verify the integrity of incoming data. Beurer-Kellner et al. [2025] propose a six architectural design patterns (action-selector, plan-then-execute, map-reduce, dual LLM, code-then-execute, and context-minimization) that secure LLM agents against prompt injection attacks. These patterns restrict an agent’s ability to process untrusted input with some trade-offs in agent flexibility.

Overall, most existing defenses are probabilistic and can be bypassed [Debenedetti et al., 2025, Costa et al., 2025]. Retrospective systems are needed to identify attackers, yet cross-service threat intelligence for large-scale prompt injection attacks correlation remains unexplored.

¹We cite the peer-reviewed conference version. An earlier preprint is available on arXiv.

4.3 Discussion

Our study has limitations similar to those in any research. Synthetic paraphrasing and word substitution may yield varying results with different LLMs and prompts. The effectiveness of the **BinaryShield**’s PII redaction module depends on the accuracy of detection methods. Residual PII may remain in prompts. Our results rely on specific embedding models, `ModernBert` (open-source) [Warner et al., 2025, Gill et al., 2025] and `OpenAI text-embedding-3-large` (proprietary). Thus, performance may vary with other models. We determined optimal Hamming distance thresholds through search on our datasets. However, these thresholds may not generalize to other attack distributions or organizational contexts. All experiments contain English prompts. Future work should explore cross-lingual attack detection and domain-specific technical prompts. We depend on computational non invertibility and differential privacy guarantees. The evaluation does not assess resistance to reconstruction attacks, which represent an orthogonal concern to current focus of the paper.

Noise can be added to the fingerprint through various differential privacy mechanisms [Warner, 1965, Wang et al., 2017, Bhowmick et al., 2018, Erlingsson et al., 2014, Feyisetan and Kasiviswanathan, 2021, Vadhan and Wang, 2021, Carvalho et al., 2021, Bollegala et al., 2023, Xie et al., 2024, Meehan et al., 2022, Asi et al., 2022, Du et al., 2023, Bittau et al., 2017, Fanti et al., 2016, Hsu et al., 2014, Near and Abuah, 2021, Fioretto et al., 2024, Dwork et al., 2014, Balle and Wang, 2018, Ding et al., 2017, Hu et al., 2024]. **BinaryShield** utilizes foundational work of Randomized Response mechanism [Warner, 1965]. Assessing the impact of other DP mechanisms and global differential privacy on the overall privacy guarantees is an important direction for future research. We did not formulate the privacy utility trade off as an optimization problem. Readers may consult existing literature on this topic [Near and Abuah, 2021, Wang et al., 2017, Dwork et al., 2014, Fioretto et al., 2024]. However, in our experiments, we empirically evaluated conditions ranging from extreme privacy, where accuracy approaches zero, to moderate and weak privacy. Each organization has specific privacy policies, and we do not recommend a particular differential privacy budget. Organizations should work with their privacy teams to select an appropriate budget based on their guidelines. Note we do not claim any novelty in the individual techniques used in **BinaryShield**. *Our primary contribution is the proposal of the first threat intelligence system for prompt injection threat correlation. We integrate insights from data anonymization, natural language processing, quantization, and differential privacy to design a practical and deployable threat intelligence system.* This work constitutes an initial step in the field, and we hope it will inspire further research in cross-service threat intelligence for LLM misuse.

5 Conclusion

The proliferation of LLMs across enterprise services has created an unprecedented security challenge: organizations operate multiple LLM services with billions of daily queries, yet regulatory boundaries prevent these services from sharing critical threat intelligence about prompt injection attacks. This fragmentation leaves each service vulnerable to attacks that may have already been detected elsewhere within the same organization, creating a fundamental gap in collective defense capabilities.

BinaryShield addresses this critical vulnerability by introducing the first privacy-preserving fingerprinting mechanism specifically designed for prompt injection threat intelligence. Through a carefully orchestrated pipeline combining PII redaction, semantic embedding, binary quantization, and randomized response, **BinaryShield** generates non-invertible fingerprints that can be safely shared across compliance boundaries while preserving the semantic characteristics necessary for effective threat correlation. When compared to `SimHash`, the privacy-preserving baseline, **BinaryShield** demonstrates superior robustness. The operational efficiency gains are equally compelling.

The implications of this work extend beyond immediate operational benefits. As LLM-based systems become critical infrastructure across finance, healthcare, and government services, the attack surface for prompt injection continues to expand exponentially. The emergence of autonomous agents and MCP servers further amplifies these risks, potentially enabling attacks that cascade from text manipulation to arbitrary code execution and system compromise. **BinaryShield** establishes the foundational infrastructure for collaborative defense against these evolving threats, creating a pathway toward industry-wide threat intelligence feeds analogous to existing malware signature ecosystems.

References

S. Abdelnabi, A. Fay, G. Cherubin, A. Salem, M. Fritz, and A. Paverd. Get My Drift? Catching LLM Task Drift with Activation Deltas. In *2025 IEEE Conference on Secure and Trustworthy Machine Learning (SaTML)*, pages 43–67, 2025a. doi: 10.1109/SaTML64287.2025.00011.

S. Abdelnabi, A. Fay, A. Salem, E. Zverev, K.-C. Liao, C.-H. Liu, C.-C. Kuo, J. Weigend, D. Manlangit, A. Apostolov, H. Umair, J. Donato, M. Kawakita, A. Mahboob, T. H. Bach, T.-H. Chiang, M. Cho, H. Choi, B. Kim, H. Lee, B. Pannell, C. McCauley, M. Russinovich, A. Paverd, and G. Cherubin. LLMail-Inject: A Dataset from a Realistic Adaptive Prompt Injection Challenge, 2025b. URL <https://arxiv.org/abs/2506.09956>.

H. Asi, V. Feldman, and K. Talwar. Optimal Algorithms for Mean Estimation under Local Differential Privacy. In *International Conference on Machine Learning*, pages 1046–1056. PMLR, 2022.

B. Balle and Y.-X. Wang. Improving the Gaussian Mechanism for Differential Privacy: Analytical Calibration and Optimal Denoising. In J. Dy and A. Krause, editors, *Proceedings of the 35th International Conference on Machine Learning*, volume 80 of *Proceedings of Machine Learning Research*, pages 394–403. PMLR, 10–15 Jul 2018. URL <https://proceedings.mlr.press/v80/balle18a.html>.

L. Beurer-Kellner, B. Buesser, A.-M. Creu, E. Debenedetti, D. Dobos, D. Fabian, M. Fischer, D. Froelicher, K. Grosse, D. Naeff, E. Ozoani, A. Paverd, F. Tramèr, and V. Volhejn. Design Patterns for Securing LLM Agents against Prompt Injections, 2025. URL <https://arxiv.org/abs/2506.08837>.

A. Bhowmick, J. Duchi, J. Freudiger, G. Kapoor, and R. Rogers. Protection Against Reconstruction and Its Applications in Private Federated Learning. *arXiv preprint arXiv:1812.00984*, 2018.

A. Bittau, U. Erlingsson, P. Maniatis, I. Mironov, A. Raghunathan, D. Lie, M. Rudominer, U. Kode, J. Tinnis, and B. Seefeld. Prochlo: Strong Privacy for Analytics in the Crowd. In *Proceedings of the 26th Symposium on Operating Systems Principles*, SOSP ’17, page 441–459, New York, NY, USA, 2017. Association for Computing Machinery. ISBN 9781450350853. doi: 10.1145/3132747.3132769. URL <https://doi.org/10.1145/3132747.3132769>.

D. Bollegala, S. Otake, T. Machide, and K.-i. Kawarabayashi. A Neighbourhood-Aware Differential Privacy Mechanism for Static Word Embeddings. In *Findings of the Association for Computational Linguistics: IJCNLP-AACL 2023 (Findings)*, pages 65–79, 2023.

B. Bullwinkel, M. Russinovich, A. Salem, S. Zanella-Béguelin, D. Jones, G. Severi, E. Kim, K. Hines, A. Minnich, Y. Zunger, et al. A Representation Engineering Perspective on the Effectiveness of Multi-Turn Jailbreaks. *arXiv preprint arXiv:2507.02956*, 2025.

R. S. Carvalho, T. Vasiloudis, and O. Feyisetan. BRR: Preserving Privacy of Text Data Efficiently on Device. *arXiv preprint arXiv:2107.07923*, 2021.

P. Chao, A. Robey, E. Dobriban, H. Hassani, G. J. Pappas, and E. Wong. Jailbreaking Black Box Large Language Models in Twenty Queries. In *2025 IEEE Conference on Secure and Trustworthy Machine Learning (SaTML)*, pages 23–42, 2025. doi: 10.1109/SaTML64287.2025.00010.

M. Costa, B. Köpf, A. Kolluri, A. Paverd, M. Russinovich, A. Salem, S. Tople, L. Wutschitz, and S. Zanella-Béguelin. Securing AI Agents with Information-Flow Control, 2025. URL <https://arxiv.org/abs/2505.23643>.

E. Debenedetti, I. Shumailov, T. Fan, J. Hayes, N. Carlini, D. Fabian, C. Kern, C. Shi, A. Terzis, and F. Tramèr. Defeating Prompt Injections by Design. *CoRR*, abs/2503.18813, March 2025. URL <https://doi.org/10.48550/arXiv.2503.18813>.

G. Deng, Y. Liu, Y. Li, K. Wang, Y. Zhang, Z. Li, H. Wang, T. Zhang, and Y. Liu. MASTERKEY: Automated Jailbreaking of Large Language Model Chatbots. In *Proceedings 2024 Network and Distributed System Security Symposium*, NDSS 2024. Internet Society, 2024a. doi: 10.14722/ndss.2024.24188. URL <http://dx.doi.org/10.14722/ndss.2024.24188>.

Y. Deng, W. Zhang, S. J. Pan, and L. Bing. Multilingual Jailbreak Challenges in Large Language Models. In *The Twelfth International Conference on Learning Representations*, 2024b. URL <https://openreview.net/forum?id=vESNKdEMGp>.

B. Ding, J. Kulkarni, and S. Yekhanin. Collecting Telemetry Data Privately. In I. Guyon, U. V. Luxburg, S. Bengio, H. Wallach, R. Fergus, S. Vishwanathan, and R. Garnett, editors, *Advances in Neural Information Processing Systems*, volume 30. Curran Associates, Inc., 2017. URL https://proceedings.neurips.cc/paper_files/paper/2017/file/253614bbac999b38b5b60cae531c4969-Paper.pdf.

M. Du, X. Yue, S. S. Chow, and H. Sun. Sanitizing Sentence Embeddings (and Labels) for Local Differential Privacy. In *Proceedings of the ACM Web Conference 2023*, pages 2349–2359, 2023.

C. Dwork, A. Roth, et al. The Algorithmic Foundations of Differential Privacy. *Foundations and trends® in theoretical computer science*, 9(3–4):211–407, 2014.

U. Erlingsson, V. Pihur, and A. Korolova. RAPPOR: Randomized Aggregatable Privacy-Preserving Ordinal Response. In *Proceedings of the 2014 ACM SIGSAC Conference on Computer and Communications Security*, CCS ’14, page 1054–1067, New York, NY, USA, 2014. Association for Computing Machinery. ISBN 9781450329576. doi: 10.1145/2660267.2660348. URL <https://doi.org/10.1145/2660267.2660348>.

G. Fanti, V. Pihur, and Ú. Erlingsson. Building a RAPPOR with the Unknown: Privacy-Preserving Learning of Associations and Data Dictionaries. *Proceedings on Privacy Enhancing Technologies*, 3:41–61, 2016.

O. Feyisetan and S. Kasiviswanathan. Private Release of Text Embedding Vectors. In *Proceedings of the First Workshop on Trustworthy Natural Language Processing*, pages 15–27, 2021.

F. Fioretto, P. Van Hentenryck, and J. Ziani. Differential Privacy Overview and Fundamental Techniques. *arXiv preprint arXiv:2411.04710*, 2024.

W. Gill, J. Cechmanek, T. Hutcherson, S. Rajamohan, J. Agarwal, M. A. Gulzar, M. Singh, and B. Dion. Advancing Semantic Caching for LLMs with Domain-Specific Embeddings and Synthetic Data, 2025. URL <https://arxiv.org/abs/2504.02268>.

K. Greshake, S. Abdelnabi, S. Mishra, C. Endres, T. Holz, and M. Fritz. Not What You’ve Signed Up For: Compromising Real-World LLM-Integrated Applications with Indirect Prompt Injection. In *Proceedings of the 16th ACM Workshop on Artificial Intelligence and Security*, AISec ’23, page 79–90, New York, NY, USA, 2023. Association for Computing Machinery. ISBN 9798400702600. doi: 10.1145/3605764.3623985. URL <https://doi.org/10.1145/3605764.3623985>.

K. Hines, G. Lopez, M. Hall, F. Zarfati, Y. Zunger, and E. Kiciman. Defending Against Indirect Prompt Injection Attacks With Spotighting. In R. Allen, S. Samtani, E. Raff, and E. M. Rudd, editors, *Proceedings of the Conference on Applied Machine Learning in Information Security (CAMLIS 2024)*, Arlington, Virginia, USA, October 24-25, 2024, volume 3920 of *CEUR Workshop Proceedings*, pages 48–62. CEUR-WS.org, 2024. URL <https://ceur-ws.org/Vol-3920/paper03.pdf>.

J. Hsu, M. Gaboardi, A. Haeberlen, S. Khanna, A. Narayan, B. C. Pierce, and A. Roth. Differential Privacy: An Economic Method for Choosing Epsilon. In *2014 IEEE 27th Computer Security Foundations Symposium*, pages 398–410. IEEE, 2014.

Y. Hu, F. Wu, Q. Li, Y. Long, G. M. Garrido, C. Ge, B. Ding, D. Forsyth, B. Li, and D. Song. SoK: Privacy-Preserving Data Synthesis. In *2024 IEEE Symposium on Security and Privacy (SP)*, pages 4696–4713, 2024. doi: 10.1109/SP54263.2024.00002.

Y. Huang, S. Gupta, M. Xia, K. Li, and D. Chen. Catastrophic Jailbreak of Open-source LLMs via Exploiting Generation. In *The Twelfth International Conference on Learning Representations*, 2024. URL <https://openreview.net/forum?id=r42tSSCHPh>.

H. Li, M. Xu, and Y. Song. Sentence embedding leaks more information than you expect: Generative embedding inversion attack to recover the whole sentence. In *Findings of the Association for Computational Linguistics: ACL 2023*, pages 14022–14040, 2023.

V. G. Li, M. Dunn, P. Pearce, D. McCoy, G. M. Voelker, and S. Savage. Reading the tea leaves: A comparative analysis of threat intelligence. In *28th USENIX Security Symposium (USENIX Security 19)*, pages 851–867, Santa Clara, CA, Aug. 2019. USENIX Association. ISBN 978-1-939133-06-9. URL <https://www.usenix.org/conference/usenixsecurity19/presentation/li>.

X. Liu, N. Xu, M. Chen, and C. Xiao. AutoDAN: Generating Stealthy Jailbreak Prompts on Aligned Large Language Models. In *The Twelfth International Conference on Learning Representations*, 2024. URL <https://openreview.net/forum?id=7Jwpw4qKkb>.

Y. Liu, Y. Jia, J. Jia, D. Song, and N. Z. Gong. DataSentinel: A Game-Theoretic Detection of Prompt Injection Attacks. In *2025 IEEE Symposium on Security and Privacy (SP)*, pages 2190–2208. IEEE, 2025.

G. S. Manku, A. Jain, and A. Das Sarma. Detecting near-duplicates for web crawling. In *Proceedings of the 16th International Conference on World Wide Web*, WWW '07, page 141–150, New York, NY, USA, 2007. Association for Computing Machinery. ISBN 9781595936547. doi: 10.1145/1242572.1242592. URL <https://doi.org/10.1145/1242572.1242592>.

C. Meehan, K. Mrini, and K. Chaudhuri. Sentence-level Privacy for Document Embeddings. In *Proceedings of the 60th Annual Meeting of the Association for Computational Linguistics (Volume 1: Long Papers)*, pages 3367–3380, 2022.

Microsoft. Home - microsoft presidio. URL <https://microsoft.github.io/presidio/>. [Online; accessed 2025-08-24].

J. P. Near and C. Abuah. *Programming Differential Privacy*, volume 1. 2021. URL <https://programming-dp.com/>.

T. H. News. Zero-Click AI Vulnerability Exposes Microsoft 365 Copilot Data Without User Interaction — thehackernews.com. <https://thehackernews.com/2025/06/zero-click-ai-vulnerability-exposes.html>. [Accessed 11-08-2025].

OWASP2025. LLM08:2025 Vector and Embedding Weaknesses. <https://genai.owasp.org/11mrisk/llm082025-vector-and-embedding-weaknesses/>, 2025. [Accessed 11-08-2025].

M. Russinovich, A. Salem, and R. Eldan. Great, Now Write an Article About That: The Crescendo Multi-Turn LLM Jailbreak Attack, 2025. URL <https://arxiv.org/abs/2404.01833>.

X. Shen, Z. Chen, M. Backes, Y. Shen, and Y. Zhang. "Do Anything Now": Characterizing and Evaluating In-The-Wild Jailbreak Prompts on Large Language Models. In *Proceedings of the 2024 on ACM SIGSAC Conference on Computer and Communications Security*, CCS '24, page 1671–1685, New York, NY, USA, 2024. Association for Computing Machinery. ISBN 9798400706363. doi: 10.1145/3658644.3670388. URL <https://doi.org/10.1145/3658644.3670388>.

A. Tragoudaras, T. Aslanidis, E. G. Lionis, M. Orozco González, and P. Eustratiadis. Information leakage of sentence embeddings via generative embedding inversion attacks. In *Proceedings of the 48th International ACM SIGIR Conference on Research and Development in Information Retrieval*, pages 3234–3243, 2025.

S. Vadhan and T. Wang. Concurrent Composition of Differential Privacy. In *Theory of Cryptography Conference*, pages 582–604, 2021.

P. Walsh. AI Systems And Vector Databases Are Generating New Privacy Risks — forbes.com. <https://www.forbes.com/councils/forbestechcouncil/2023/11/02/ai-systems-and-vector-databases-are-generating-new-privacy-risks/>. [Accessed 12-08-2025].

T. Wang, J. Blocki, N. Li, and S. Jha. Locally Differentially Private Protocols for Frequency Estimation. In *26th USENIX Security Symposium (USENIX Security 17)*, pages 729–745, Vancouver, BC, Aug. 2017. USENIX Association. ISBN 978-1-931971-40-9. URL <https://www.usenix.org/conference/usenixsecurity17/technical-sessions/presentation/wang-tianhao>.

B. Warner, A. Chaffin, B. Clavié, O. Weller, O. Hallström, S. Taghadouini, A. Gallagher, R. Biswas, F. Ladhak, T. Aarsen, G. T. Adams, J. Howard, and I. Poli. Smarter, Better, Faster, Longer: A Modern Bidirectional Encoder for Fast, Memory Efficient, and Long Context Finetuning and Inference. In W. Che, J. Nabende, E. Shutova, and M. T. Pilehvar, editors, *Proceedings of the 63rd Annual Meeting of the Association for Computational Linguistics (Volume 1: Long Papers)*, pages 2526–2547, Vienna, Austria, July 2025. Association for Computational Linguistics. ISBN 979-8-89176-251-0. doi: 10.18653/v1/2025.acl-long.127. URL <https://aclanthology.org/2025.acl-long.127/>.

S. L. Warner. Randomized Response: A Survey Technique for Eliminating Evasive Answer Bias. *Journal of the American statistical association*, 60(309):63–69, 1965.

A. Wei, N. Haghtalab, and J. Steinhardt. Jailbroken: How Does LLM Safety Training Fail? In *Thirty-seventh Conference on Neural Information Processing Systems*, 2023. URL <https://openreview.net/forum?id=jA235JGM09>.

C. Xie, Z. Lin, A. Backurs, S. Gopi, D. Yu, H. A. Inan, H. Nori, H. Jiang, H. Zhang, Y. T. Lee, et al. Differentially Private Synthetic Data via Foundation Model APIs 2: Text. In *International Conference on Machine Learning*, pages 54531–54560. PMLR, 2024.

Z. Yang, M. Backes, Y. Zhang, and A. Salem. SOS! Soft Prompt Attack Against Open-Source Large Language Models. *CoRR*, abs/2407.03160, 2024. URL <https://doi.org/10.48550/arXiv.2407.03160>.

J. Yi, Y. Xie, B. Zhu, E. Kiciman, G. Sun, X. Xie, and F. Wu. Benchmarking and Defending against Indirect Prompt Injection Attacks on Large Language Models. In *Proceedings of the 31st ACM SIGKDD Conference on Knowledge Discovery and Data Mining V.I*, KDD ’25, page 1809–1820, New York, NY, USA, 2025. Association for Computing Machinery. ISBN 9798400712456. doi: 10.1145/3690624.3709179. URL <https://doi.org/10.1145/3690624.3709179>.

Z. Yuan, Z. Xiong, Y. Zeng, N. Yu, R. Jia, D. Song, and B. Li. RigorLLM: Resilient Guardrails for Large Language Models against Undesired Content. In *Forty-first International Conference on Machine Learning*, 2024. URL <https://openreview.net/forum?id=QAGRiC3FS>.

Y. Zhang, N. Carlini, and D. Ippolito. Effective Prompt Extraction from Language Models. In *First Conference on Language Modeling*, 2024. URL <https://openreview.net/forum?id=0o95CVdNuz>.

W. Zhao, X. Ren, J. Hessel, C. Cardie, Y. Choi, and Y. Deng. WildChat: 1M ChatGPT Interaction Logs in the Wild. In *The Twelfth International Conference on Learning Representations*, 2024. URL <https://openreview.net/forum?id=B18u7ZR1bM>.

A. Zou, Z. Wang, N. Carlini, M. Nasr, J. Z. Kolter, and M. Fredrikson. Universal and Transferable Adversarial Attacks on Aligned Language Models, 2023. URL <https://arxiv.org/abs/2307.15043>.

A. Zou, L. Phan, J. Wang, D. Duenas, M. Lin, M. Andriushchenko, J. Z. Kolter, M. Fredrikson, and D. Hendrycks. Improving Alignment and Robustness with Circuit Breakers. In *The Thirty-eighth Annual Conference on Neural Information Processing Systems*, 2024. URL <https://openreview.net/forum?id=IbIB8SBKFV>.